This journal is © The Owner Societies 2012

Peptide Loop and α-Helix N-terminus Serving as Alternative Electron Hopping Relays in Proteins

Boran Han,[†,‡] Xiaohua Chen,[†,§] Jing Zhao,[†] and Yuxiang Bu [*,†]

[†] *School of Chemistry and Chemical Engineering, Shandong University, Jinan, 250100, P. R. China*

[‡] *Physics School, Shandong University, Jinan, 250100, P. R. China*

[§] *Department of Chemistry, Chongqing University, Chongqing, 400030, P. R. China*

Corresponding Author: *Dr. Prof. Yuxiang Bu, byx@sdu.edu.cn*

Contents for Supplementary Materials

1. Relevant Calculational Data and Spin Density Distributions for Three Kinds of Model Oligopeptides

2. Calculational Details for Local Dipole Moments

3. Molecular Configurations of an Arbitrary Peptide Chain Used in Figure 6

4. The Calculated Data for α-Helices

5. Geometries and Spin Density Distributions of All α-Helices

1. Relevant Calculational Data and Spin Density Distributions of Three Kinds of Model Oligopeptides

Structure *a* (H-(Gly)$_n$-CH$_3$)

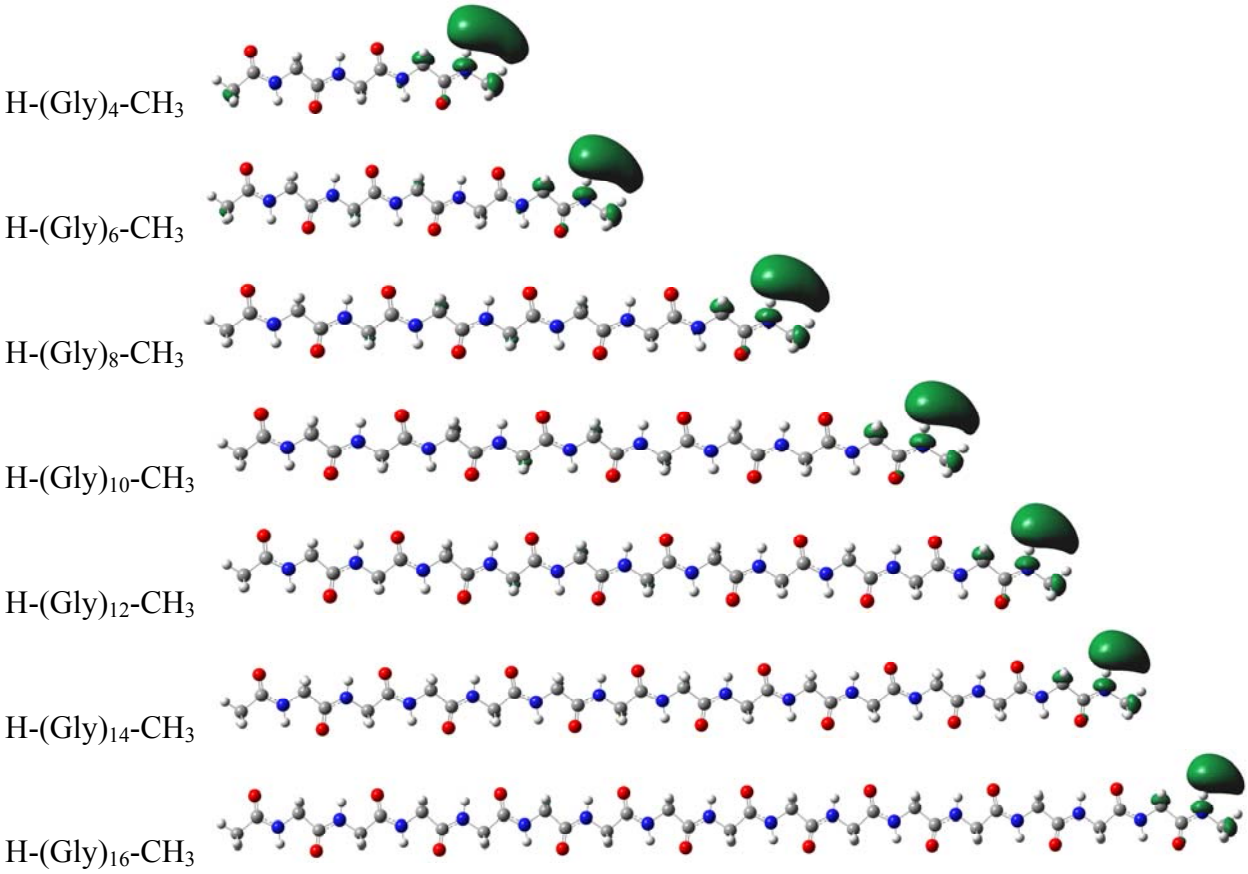

Figure S1. The spin density distributions of a vertically-bound excess electron at the N-terminal of the optimized neutral oligopeptides (Structure ***a***, H-(Gly)$_n$-CH$_3$, n=4, 6, 8,10, 12, 14, and 16)

Table S1. The HOMO (eV), LUMO (eV), Gaps (eV), and Dipole Moments (Debye) of the optimized neutral oligopeptides (Structure ***a***, H-(Gly)$_n$-CH$_3$, n=4, 6, 8, 10, 12, 14, and 16) and the SOMO (vertical, eV) after Adding An Electron Vertically

Structure ***a*** (optimized)	HOMO	LUMO	Gaps	Dipole moments	SOMO (vertical)
H-(Gly)$_4$-CH$_3$	-6.82	-0.89	5.94	8.16	0.896
H-(Gly)$_6$-CH$_3$	-6.77	-0.98	5.79	13.09	0.689
H-(Gly)$_8$-CH$_3$	-6.74	-1.02	5.72	18.12	0.533
H-(Gly)$_{10}$-CH$_3$	-6.72	-1.04	5.68	23.19	0.408
H-(Gly)$_{12}$-CH$_3$	-6.71	-1.05	5.66	28.27	0.308
H-(Gly)$_{14}$-CH$_3$	-6.71	-1.06	5.65	33.36	0.225
H-(Gly)$_{16}$-CH$_3$	-6.69	-1.07	5.62	38.46	0.158

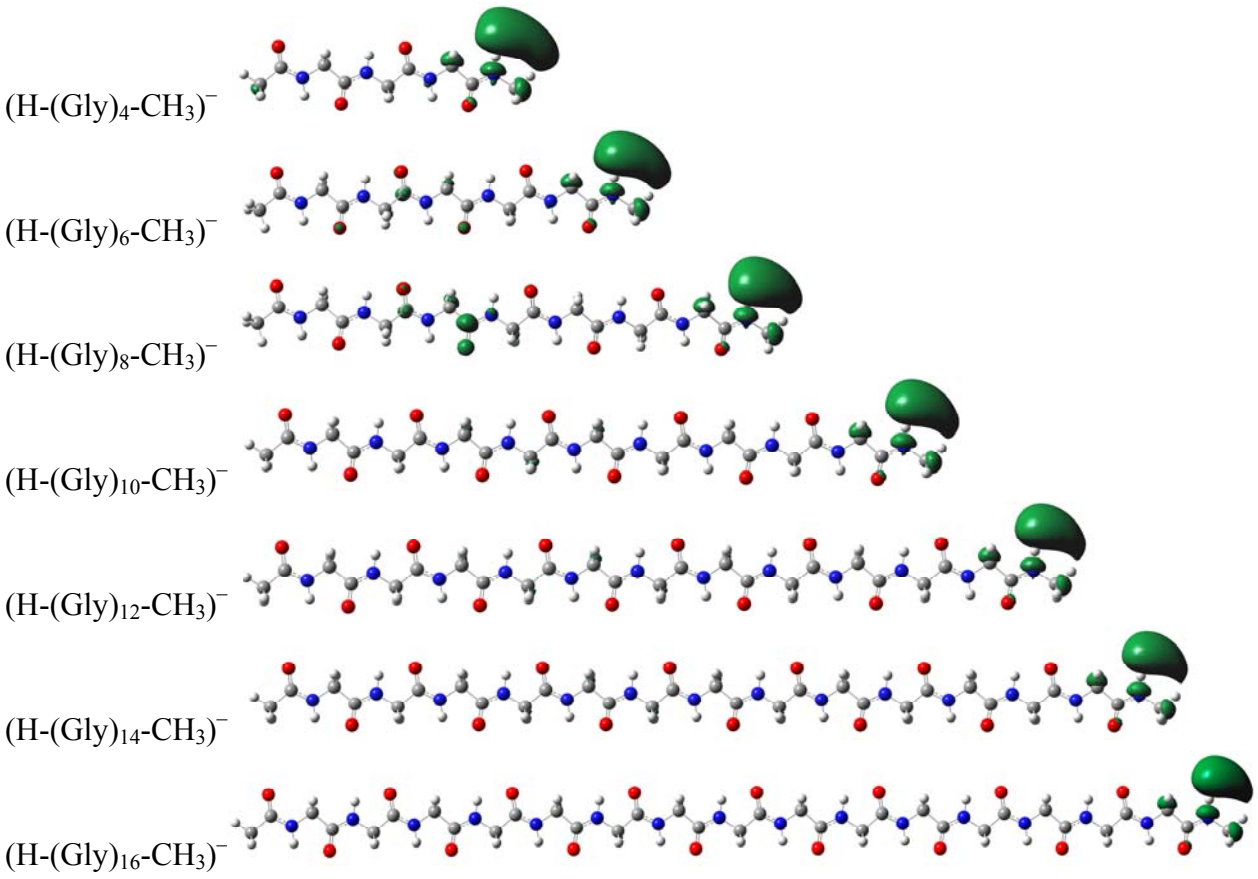

Figure S2. The spin density distributions of the optimized one-electron-bound structures of oligopeptides (Structure ***a***, $(H\text{-}(Gly)_n\text{-}CH_3)^-$, n=4, 6, 8,10, 12, 14, and 16).

Table S2. The SOMO (eV) of the Optimized Anions of Oligopeptides (Structure ***a***, $H\text{-}(Gly)_n\text{-}CH_3$, n=4, 6, 8, 10, 12, 14, and 16) and The HOMO (eV), LUMO (eV), Gaps (eV), and Dipole Moments (Debye) of Their Corresponding Vertically Ionized Structures

Structure ***a*** (optimized)	SOMO (optimized)	Structure ***a*** (vertical)	HOMO	LUMO	Gaps	Dipole moments
$(H\text{-}(Gly)_4\text{-}CH_3)^-$	0.901	$H\text{-}(Gly)_4\text{-}CH_3$	-6.75	-0.99	5.76	9.17
$(H\text{-}(Gly)_6\text{-}CH_3)^-$	0.684	$H\text{-}(Gly)_6\text{-}CH_3$	-6.71	-1.05	5.66	14.03
$(H\text{-}(Gly)_8\text{-}CH_3)^-$	0.509	$H\text{-}(Gly)_8\text{-}CH_3$	-6.69	-1.08	5.61	18.88
$(H\text{-}(Gly)_{10}\text{-}CH_3)^-$	0.397	$H\text{-}(Gly)_{10}\text{-}CH_3$	-6.72	-1.10	5.68	23.19
$(H\text{-}(Gly)_{12}\text{-}CH_3)^-$	0.297	$H\text{-}(Gly)_{12}\text{-}CH_3$	-6.71	-1.11	5.66	29.24
$(H\text{-}(Gly)_{14}\text{-}CH_3)^-$	0.215	$H\text{-}(Gly)_{14}\text{-}CH_3$	-6.68	-1.12	5.56	34.31
$(H\text{-}(Gly)_{16}\text{-}CH_3)^-$	0.148	$H\text{-}(Gly)_{16}\text{-}CH_3$	-6.67	-1.13	5.54	39.38

Table S3. The Vertical Electron Affinities (VEAs, in eV) of Oligopeptides (Structure ***a***, H-$(Gly)_n$-CH_3, n=4, 6, 8, 10, 12, 14, and 16), and the Vertical Detachment Energies (VDEs, in eV) of the Corresponding One-Electron-Bound Structures, $(H\text{-}(Gly)_n\text{-}CH_3)^-$, n=4, 6, 8, 10, 12, 14, 16

Species	VEAs	Species	VDEs
H-$(Gly)_4$-CH_3	-0.019	$(H\text{-}(Gly)_4\text{-}CH_3)^-$	0.022
H-$(Gly)_6$-CH_3	0.106	$(H\text{-}(Gly)_6\text{-}CH_3)^-$	0.156
H-$(Gly)_8$-CH_3	0.192	$(H\text{-}(Gly)_8\text{-}CH_3)^-$	0.250
H-$(Gly)_{10}$-CH_3	0.257	$(H\text{-}(Gly)_{10}\text{-}CH_3)^-$	0.294
H-$(Gly)_{12}$-CH_3	0.307	$(H\text{-}(Gly)_{12}\text{-}CH_3)^-$	0.341
H-$(Gly)_{14}$-CH_3	0.348	$(H\text{-}(Gly)_{14}\text{-}CH_3)^-$	0.377
H-$(Gly)_{16}$-CH_3	0.377	$(H\text{-}(Gly)_{16}\text{-}CH_3)^-$	0.403

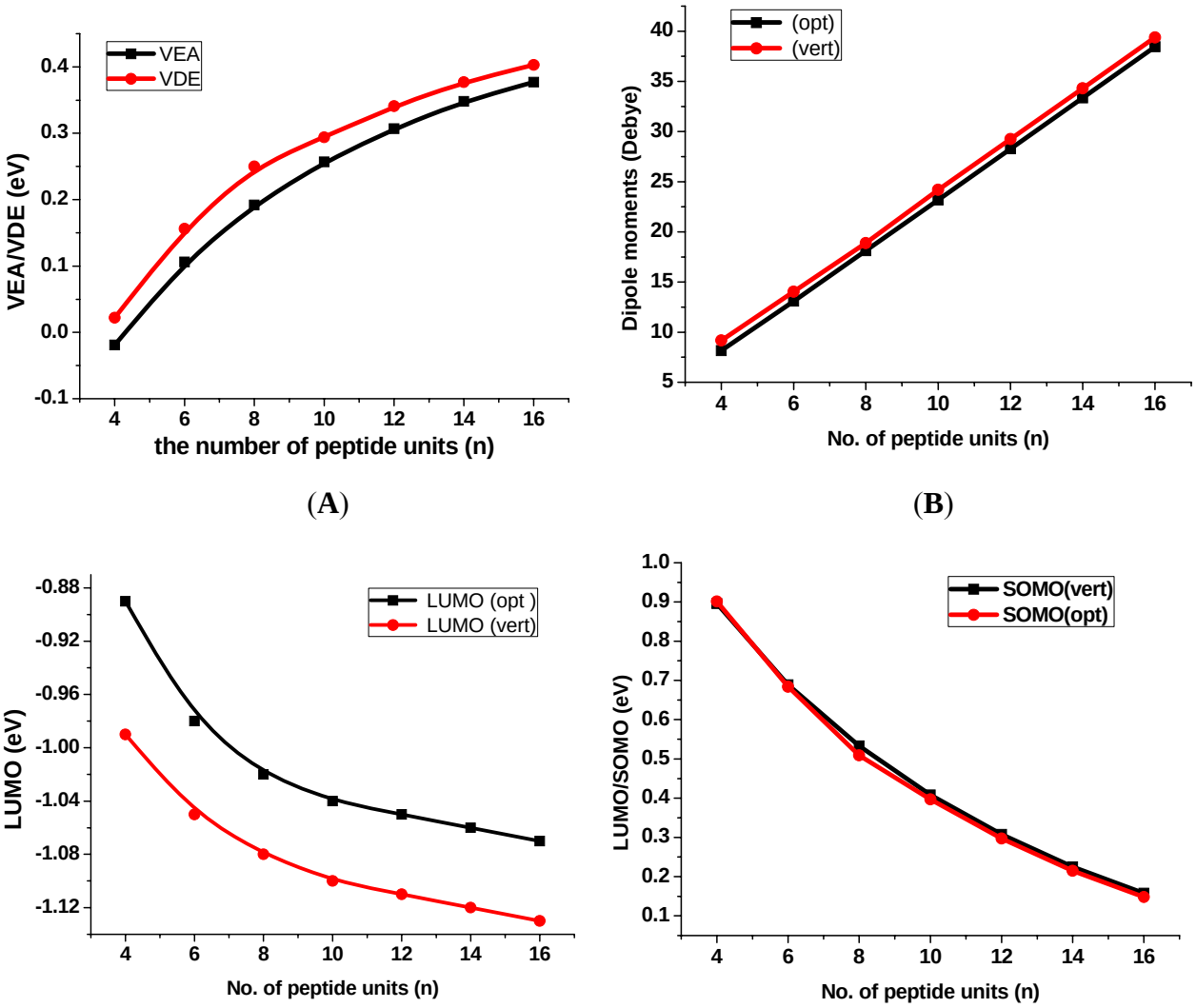

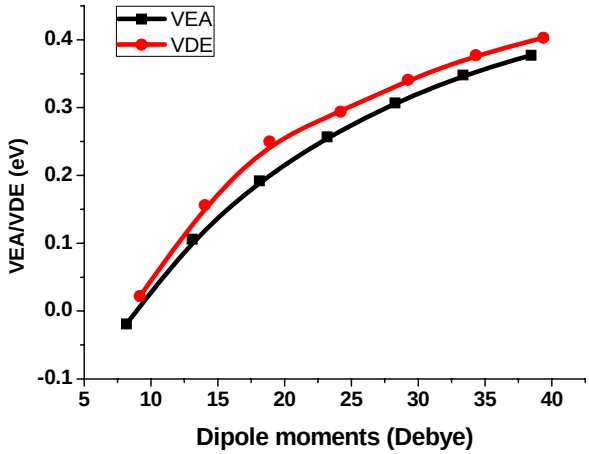

(**E**)

Figure S3. (**A**) Peptide chain length (n) dependences of VEAs of the neutral oligopeptides and VDEs of the oligopeptide anions for Structure **a** (H-(Gly)$_n$-CH$_3$, n=4, 6, 8, 10, 12, 14, and 16); (**B**) Peptide chain length (n) dependences of dipole moments of the neutral oligopeptides and the corresponding neutral geometries of the vertically ionized anions; (**C**) Peptide chain length dependences of the LUMO energies of the neutral oligopeptides and the corresponding neutral geometries of the vertically ionized anions; (**D**) Peptide chain length (n) dependences of the SOMO energies of the optimized oligopeptide anions (opt) and the anions at their corresponding optimized neutral geometries (vert); (**E**) Dependences of VEAs of the neutral oligopeptides and VDE of the oligopeptide anions on dipole moments of the optimized neutral oligopeptides and the corresponding neutral geometries after removing an electron vertically from the optimized oligopeptide anions, respectively.

Structure *b* ($^{+}NH_3$-$(Gly)_n$-CH_3)

$^{+}NH_3$-$(Gly)_4$-CH_3

$^{+}NH_3$-$(Gly)_6$-CH_3

$^{+}NH_3$-$(Gly)_8$-CH_3

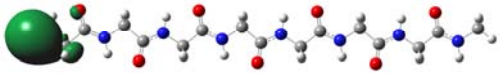

$^{+}NH_3$-$(Gly)_{10}$-CH_3

$^{+}NH_3$-$(Gly)_{12}$-CH_3

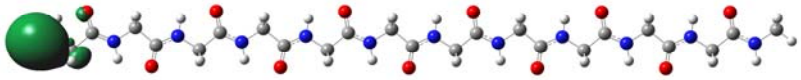

$^{+}NH_3$-$(Gly)_{14}$-CH_3

$^{+}NH_3$-$(Gly)_{16}$-CH_3

Figure S4. The spin density distributions of a vertically-captured excess electron at the $-NH_3^{+}$ group of the N-terminal oligopeptides (Structure ***b***), $^{+}NH_3$-$(Gly)_n$-CH_3 (n=4, 6, 8,10, 12, 14, and 16).

Table S4. The HOMO (eV), LUMO (eV), Gaps (eV), and Dipole Moments (Debye) of the N-terminal oligopeptides (Structure ***b***), $^{+}NH_3$-$(Gly)_n$-CH_3 (n=4, 6, 8, 10, 12, 14, and 16) and the SOMO (vertical, eV) after Adding An Electron Vertically

Structure ***b*** (optimized)	HOMO	LUMO	Gaps	Dipole Moments	SOMO (vertical)
$^{+}NH_3$-$(Gly)_4$-CH_3	-9.68	-4.86	4.83	15.97	-1.967
$^{+}NH_3$-$(Gly)_6$-CH_3	-8.93	-4.78	4.15	27.41	-1.894
$^{+}NH_3$-$(Gly)_8$-CH_3	-8.54	-4.74	3.80	39.33	-1.860
$^{+}NH_3$-$(Gly)_{10}$-CH_3	-8.31	-4.72	3.59	51.43	-1.841
$^{+}NH_3$-$(Gly)_{12}$-CH_3	-8.15	-4.71	3.44	63.60	-1.828
$^{+}NH_3$-$(Gly)_{14}$-CH_3	-8.03	-4.70	3.34	75.81	-1.820
$^{+}NH_3$-$(Gly)_{16}$-CH_3	-7.95	-4.69	3.26	88.04	-1.814

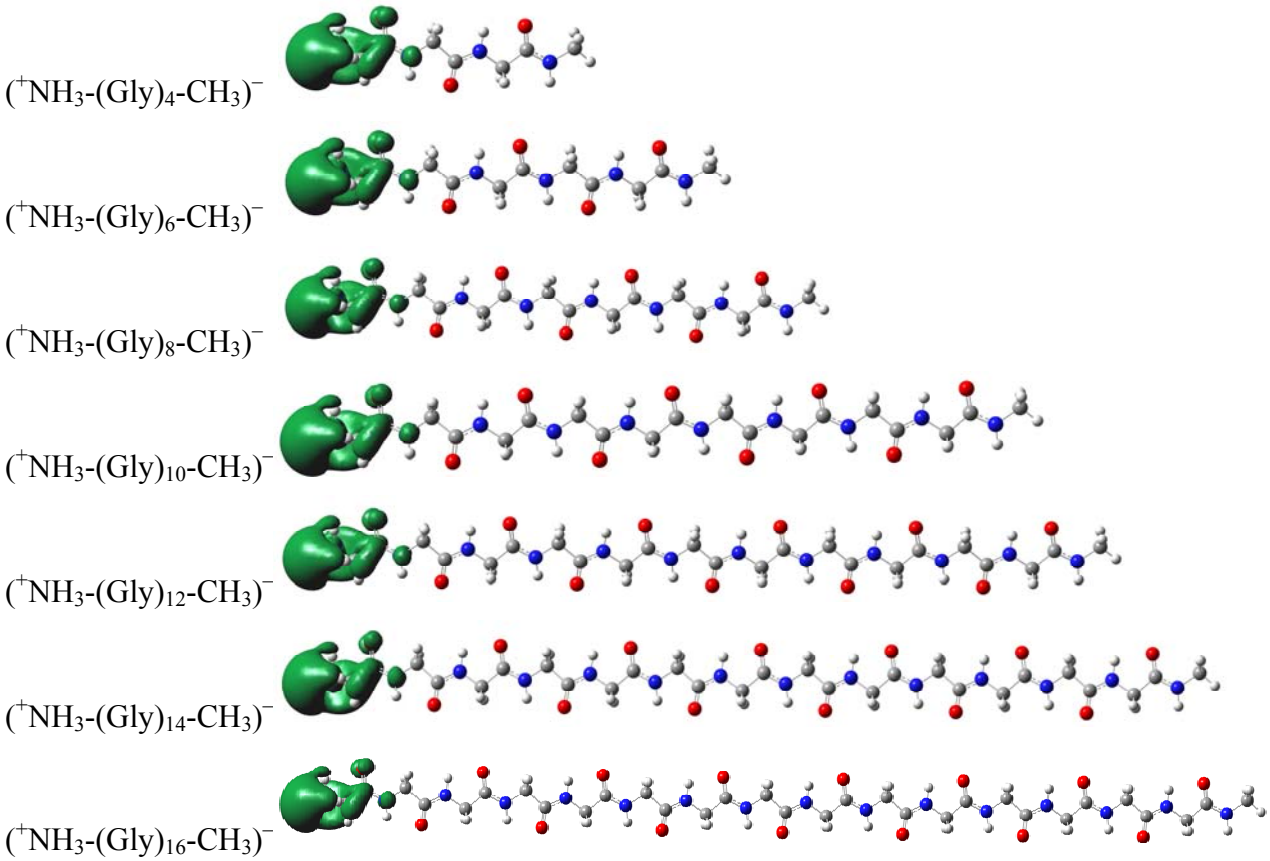

Figure S5. The spin density distributions of the optimized one-electron-bound structures of the N-terminal oligopeptides (Structure ***b***, $(^{+}NH_3\text{-}(Gly)_n\text{-}CH_3)^{-}$, n=4, 6, 8,10, 12, 14, and 16).

Table S5. The SOMO (neutral, eV) of the Optimized One-Electron-Bound Structures of the N-terminal oligopeptides for Structure ***b***, $(^{+}NH_3\text{-}(Gly)_n\text{-}CH_3)^{-}$, n=4, 6, 8, 10, 12, 14, and 16) and The HOMO (eV), LUMO (eV), Gaps (eV), and Dipole Moments (Debye) of Their Corresponding Vertically Ionized Structures

Species (optimized)	SOMO (optimized)	Species (vertical)	HOMO	LUMO	Gaps	Dipole moments
$(^{+}NH_3\text{-}(Gly)_4\text{-}CH_3)^{-}$	-2.446	$^{+}NH_3\text{-}(Gly)_4\text{-}CH_3$	-9.50	-5.59	3.91	18.49
$(^{+}NH_3\text{-}(Gly)_6\text{-}CH_3)^{-}$	-2.375	$^{+}NH_3\text{-}(Gly)_6\text{-}CH_3$	-8.82	-5.52	3.30	30.23
$(^{+}NH_3\text{-}(Gly)_8\text{-}CH_3)^{-}$	-2.334	$^{+}NH_3\text{-}(Gly)_8\text{-}CH_3$	-8.47	-5.48	2.99	42.29
$(^{+}NH_3\text{-}(Gly)_{10}\text{-}CH_3)^{-}$	-2.317	$^{+}NH_3\text{-}(Gly)_{10}\text{-}CH_3$	-8.27	-5.44	2.83	54.47
$(^{+}NH_3\text{-}(Gly)_{12}\text{-}CH_3)^{-}$	-2.309	$^{+}NH_3\text{-}(Gly)_{12}\text{-}CH_3$	-8.12	-5.42	2.68	66.69
$(^{+}NH_3\text{-}(Gly)_{14}\text{-}CH_3)^{-}$	-2.307	$^{+}NH_3\text{-}(Gly)_{14}\text{-}CH_3$	-8.01	-5.40	2.58	78.92
$(^{+}NH_3\text{-}(Gly)_{16}\text{-}CH_3)^{-}$	-2.295	$^{+}NH_3\text{-}(Gly)_{16}\text{-}CH_3$	-7.96	-5.38	2.58	91.19

Table S6. The Vertical Electron Affinities (VEAs, in eV) of the N-terminal Oligopeptides (Structure ***b***, $^{+}NH_3$-$(Gly)_n$-CH_3, n=4, 6, 8, 10, 12, 14, and 16), and the Vertical Detachment Energies (VDEs, in eV) of the Corresponding One-Electron-Bound Structures, $(^{+}NH_3$-$(Gly)_n$-$CH_3)^{-}$, n=4, 6, 8, 10, 12, 14, and 16

Species	VEA	Species	VDE
$^{+}NH_3$-$(Gly)_4$-CH_3	3.429	$(^{+}NH_3$-$(Gly)_4$-$CH_3)^{-}$	4.025
$^{+}NH_3$-$(Gly)_6$-CH_3	3.353	$(^{+}NH_3$-$(Gly)_6$-$CH_3)^{-}$	3.952
$^{+}NH_3$-$(Gly)_8$-CH_3	3.318	$(^{+}NH_3$-$(Gly)_8$-$CH_3)^{-}$	3.915
$^{+}NH_3$-$(Gly)_{10}$-CH_3	3.298	$(^{+}NH_3$-$(Gly)_{10}$-$CH_3)^{-}$	3.891
$^{+}NH_3$-$(Gly)_{12}$-CH_3	3.286	$(^{+}NH_3$-$(Gly)_{12}$-$CH_3)^{-}$	3.885
$^{+}NH_3$-$(Gly)_{14}$-CH_3	3.278	$(^{+}NH_3$-$(Gly)_{14}$-$CH_3)^{-}$	3.876
$^{+}NH_3$-$(Gly)_{16}$-CH_3	3.266	$(^{+}NH_3$-$(Gly)_{16}$-$CH_3)^{-}$	3.873

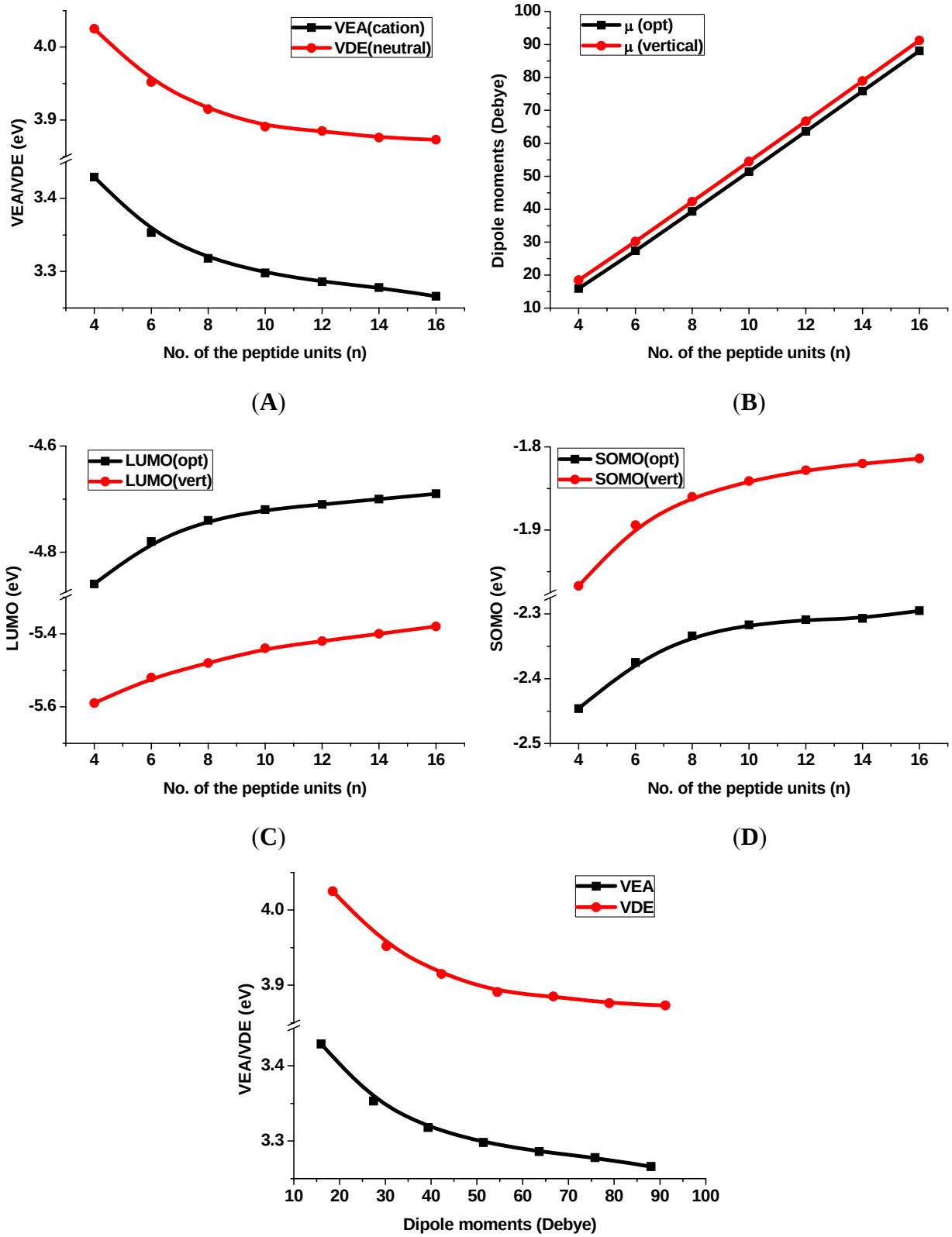

Figure S6. (**A**) Peptide chain length (n) dependences of VEAs of the N-terminal oligopeptides and VDE of their one-electron-bound derivatives for Structure **b** ($^{+}NH_3$-$(Gly)_n$-CH_3, n=4, 6, 8, 10, 12, 14, and 16); (**B**) Peptide chain length (n) dependences of dipole moments of the N-terminal oligopeptides and the corresponding geometries of the vertically ionized one-electron-bound

derivatives; (**C**) Peptide chain length (n) dependences of the LUMO energies of the N-terminal oligopeptides and the corresponding geometries of the vertically ionized one-electron-bound derivatives; (**D**) Peptide chain length (n) dependences of the SOMO energies of the optimized one-electron-bound oligopeptides (opt) and the vertically one-electron-bound N-terminal oligopeptides (vert); (**E**) Dependences of VEAs of the N-terminal oligopeptides and VDE of the one-electron-bound N-terminal oligopeptides on dipole moments of the optimized N-terminal oligopeptides and the corresponding geometries after removing an electron vertically from the optimized one-electron bound oligopeptides, respectively.

Additional Notes: It seems to be contractive to the variation of total dipole moments along with the peptide chain elongation. For the structure (**b**) series, total dipole moment noticeably increases as the peptide chain elongates, which is similar to that in the structure (**a**) series. But, total dipole moments of the structure (**b**) are also considerably larger than those of the corresponding structure (**a**) with same chain length. Actually, introduction of a $–NH_3^+$ group into the C-terminal of the peptide chain modifies the total dipole direction towards the $–NH_3^+$ group for the structure (**b**), as shown in Figure 3 in the text. Clearly, in this case, the charge Q is larger than that in the structure (**a**) and slightly decreases as the peptide chain elongates. Thus, noticeable increase of total dipole moment of the structure (**b**) should be due to the pure distance effect according to $\mu=Q\times R$. This means that these extremely large dipole moment increases do not implicate an increase of the electron binding ability of the N-terminal oligopeptides. In other words, cooperation of electrostatic attraction of $–NH_3^+$ and inhibiting effect of the local dipole (viz. the macro-dipole of the peptide chain part) are the main driving force in capturing an excess electron instead of total dipole of the structure (**b**).

Structure *c* (H-(Gly)$_n$-COOH)

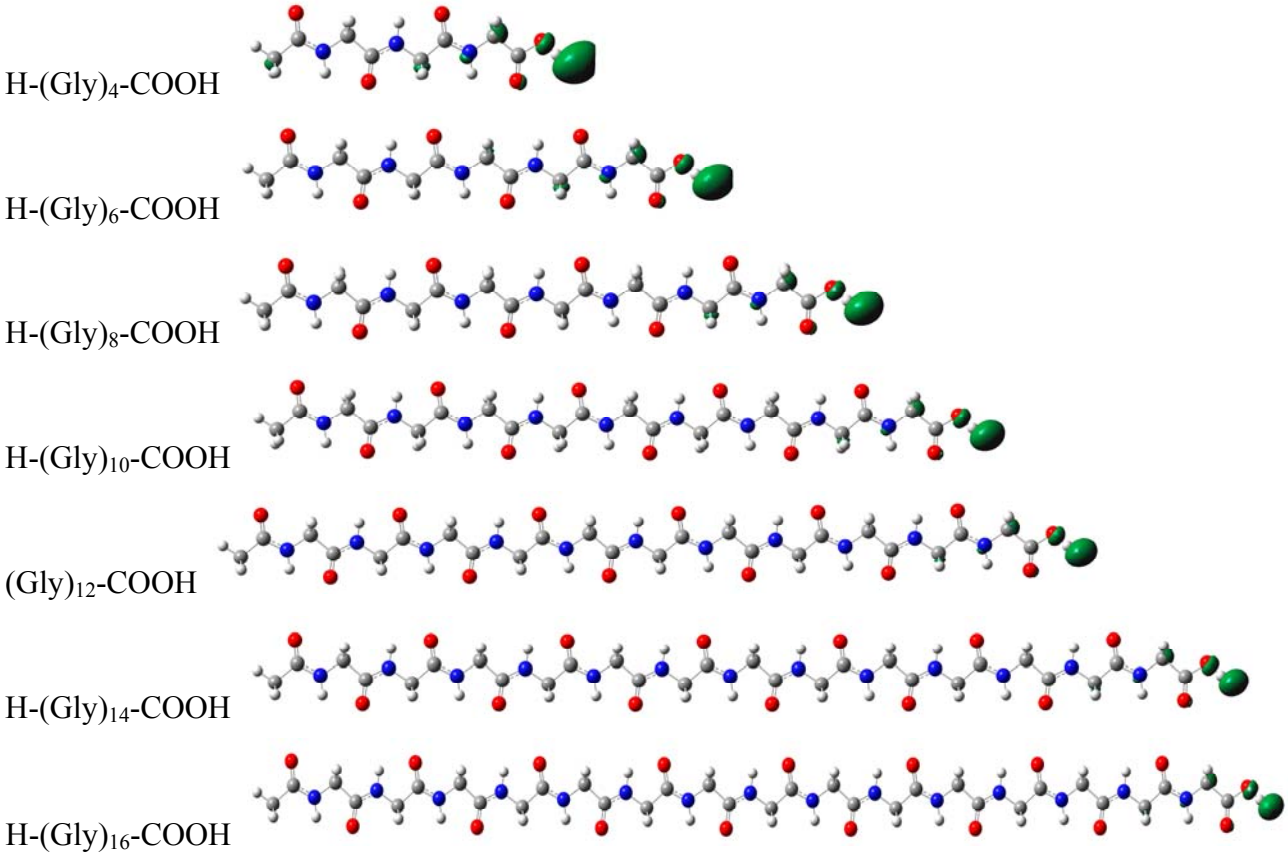

Figure S7. The spin density distributions of a vertically-captured excess electron at the C-terminal of the C-terminal oligopeptides (Structure ***c***), H-(Gly)$_n$-COOH (n=4, 6, 8,10, 12, 14, and 16).

Table S7. The HOMO (eV), LUMO (eV), Gap (eV), and Dipole moments (Debye) of the C-terminal Oligopeptides (Structure ***c***), H-(Gly)$_n$-COOH (n=4, 6, 8, 10, 12, 14, and 16) and the SOMO (vertical, eV) after Adding An Electron Vertically

Structure ***c*** (optimized)	HOMO	LUMO	Gaps	Dipole moments	SOMO (vertical)
H-(Gly)$_4$-COOH	-6.90	-1.18	5.72	6.48	0.933
H-(Gly)$_6$-COOH	-6.80	-1.29	5.50	11.19	0.714
H-(Gly)$_8$-COOH	-6.75	-1.33	5.41	16.12	0.553
H-(Gly)$_{10}$-COOH	-6.72	-1.36	5.36	21.14	0.425
H-(Gly)$_{12}$-COOH	-6.71	-1.38	5.33	26.20	0.322
H-(Gly)$_{14}$-COOH	-6.70	-1.39	5.31	31.27	0.238
H-(Gly)$_{16}$-COOH	-6.70	-1.40	5.30	36.34	0.168

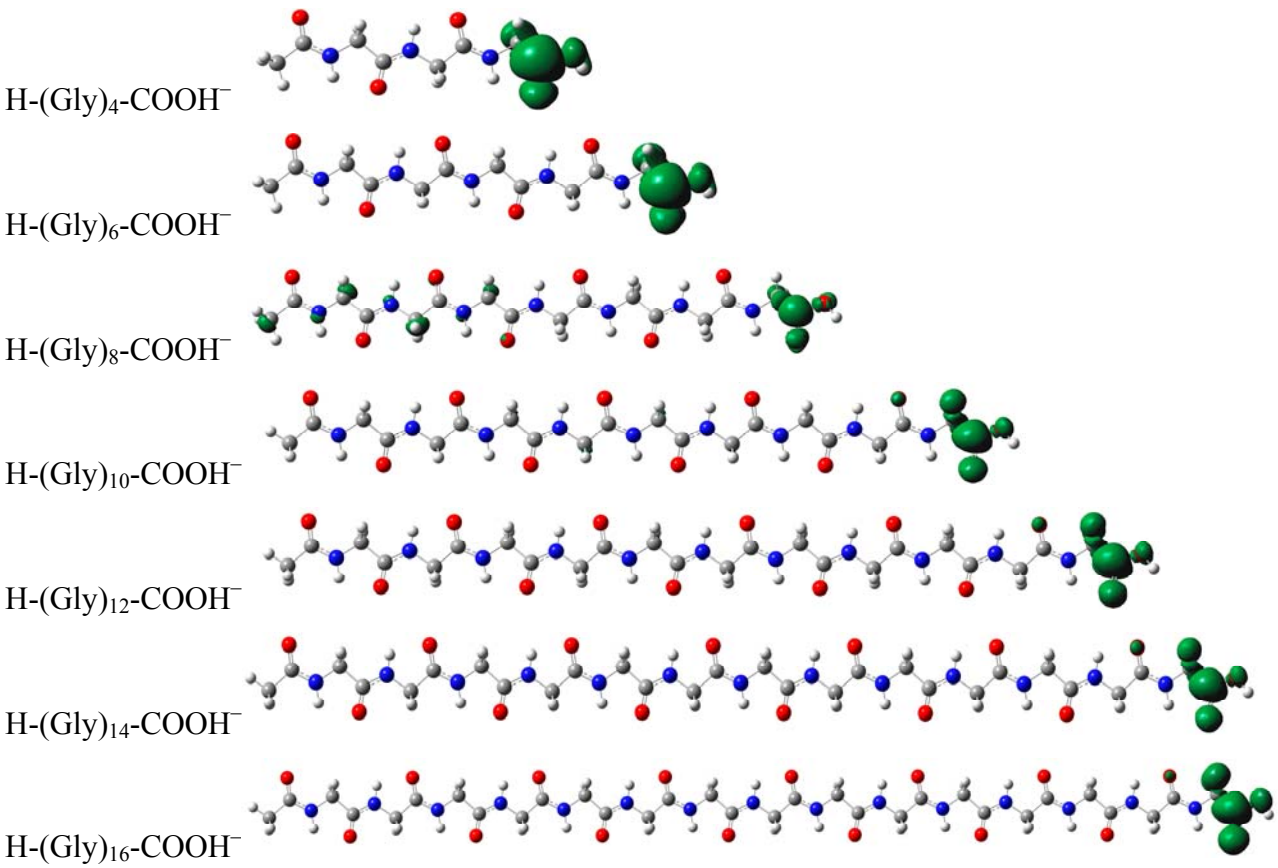

Figure S8. The spin density distributions of the optimized anionic structures of the C-terminal oligopeptides (Structure ***c***), H-Gly)$_n$-COOH$^-$ (n=4, 6, 8,10, 12, 14, and 16).

Table S8. The SOMO (eV) of the Optimized Anionic Structures of the C-terminal oligopeptides (Structure ***c***), H-(Gly)$_n$-COOH (n=4, 6, 8, 10, 12, 14, and 16) and The HOMO (eV), LUMO (eV), Gaps (eV), and Dipole Moments (Debye) of Their Vertically Ionized Structures

Structure ***c*** (optimized)	SOMO	Structure ***c*** (vertical)	HOMO	LUMO	Gaps	Dipole moments
(H-(Gly)$_4$-COOH)$^-$	1.018	H-(Gly)$_4$-COOH	-6.74	-1.93	4.81	7.40
(H-(Gly)$_6$-COOH)$^-$	0.865	H-(Gly)$_6$-COOH	-6.67	-1.98	4.67	12.39
(H-(Gly)$_8$-COOH)$^-$	0.680	H-(Gly)$_8$-COOH	-6.70	-2.03	4.66	17.39
(H-(Gly)$_{10}$-COOH)$^-$	0.533	H-(Gly)$_{10}$-COOH	-6.68	-2.00	4.68	22.50
(H-(Gly)$_{12}$-COOH)$^-$	0.414	H-(Gly)$_{12}$-COOH	-6.68	-1.98	4.70	27.63
(H-(Gly)$_{14}$-COOH)$^-$	0.316	H-(Gly)$_{14}$-COOH	-6.67	-1.96	4.71	32.78
(H-(Gly)$_{16}$-COOH)$^-$	0.221	H-(Gly)$_{16}$-COOH	-6.67	-1.94	4.73	37.95

Table S9. The Vertical Electron Affinities (VEAs, in eV) of the C-terminal Oligopeptides (Structure ***c***), H-(Gly)$_n$-COOH (n=4, 6, 8, 10, 12, 14, and 16), and the Vertical Detachment Energies (VDEs, in eV) of the Corresponding Anionic Structures, H-(Gly)$_n$-COOH$^-$ (n=4, 6, 8, 10, 12, 14, and 16)

Structure ***c***	VEAs	Structure ***c*** anions	VDEs
H-(Gly)$_4$-COOH	-0.081	H-(Gly)$_4$-COOH$^-$	0.039
H-(Gly)$_6$-COOH	0.061	H-(Gly)$_6$-COOH$^-$	0.165
H-(Gly)$_8$-COOH	0.154	H-(Gly)$_8$-COOH$^-$	0.286
H-(Gly)$_{10}$-COOH	0.222	H-(Gly)$_{10}$-COOH$^-$	0.345
H-(Gly)$_{12}$-COOH	0.274	H-(Gly)$_{12}$-COOH$^-$	0.391
H-(Gly)$_{14}$-COOH	0.314	H-(Gly)$_{14}$-COOH$^-$	0.428
H-(Gly)$_{16}$-COOH	0.347	H-(Gly)$_{16}$-COOH$^-$	0.498

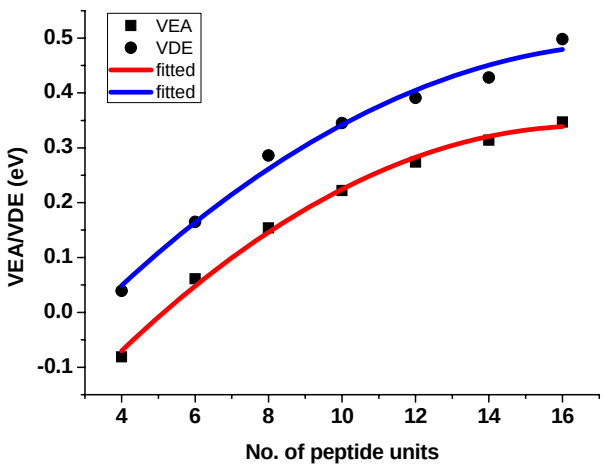

(**A**)

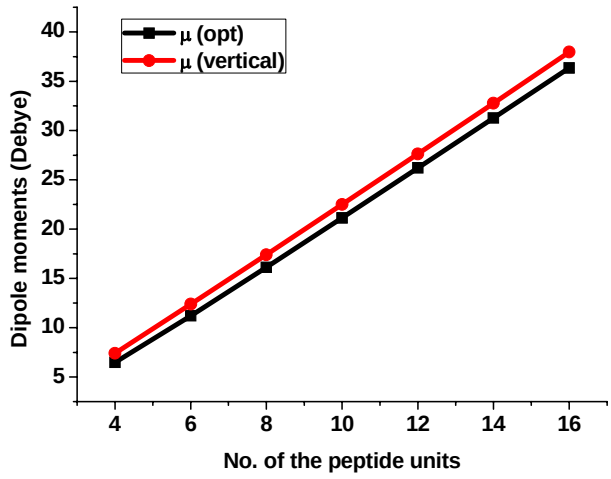

(**B**)

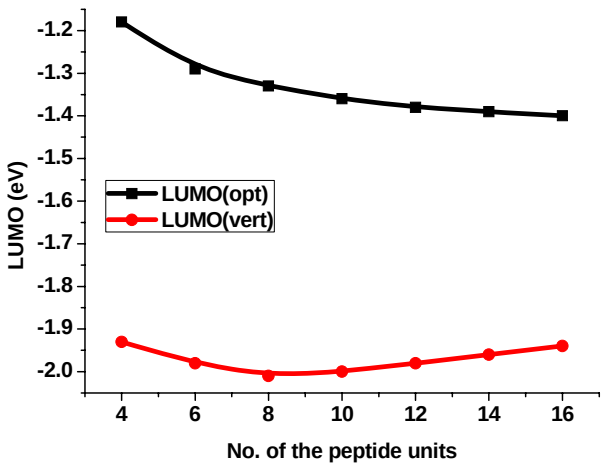

(**C**)

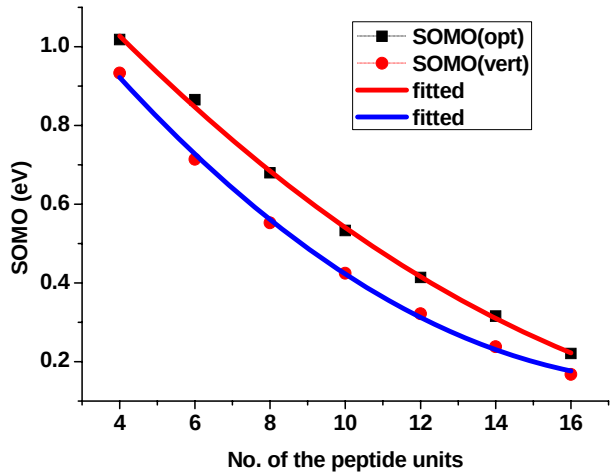

(**D**)

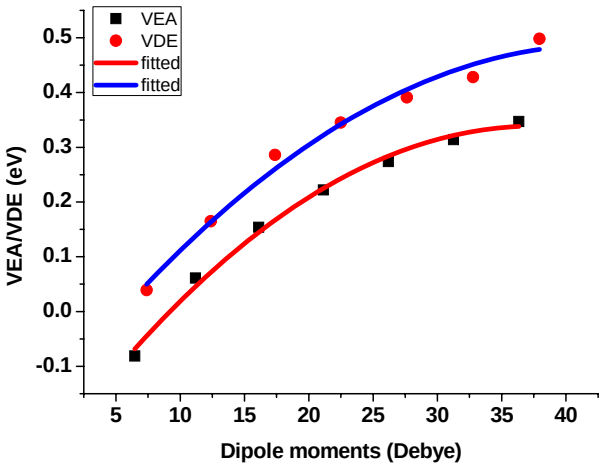

(**E**)

Figure S9. (**A**) Peptide chain length (n) dependences of VEAs of the neutral C-terminal oligopeptides and VDE of the corresponding C-terminal oligopeptide anions for Structure **c** (H-$(Gly)_n$-COOH, n=4, 6, 8, 10, 12, 14, and 16); (**B**) Peptide chain length (n) dependences of dipole moments of the neutral C-terminal oligopeptides and the corresponding neutral geometries of the vertically ionized anions; (**C**) Peptide chain length (n) dependences of the LUMO energies of the neutral C-terminal oligopeptides and the corresponding neutral geometries of the vertically ionized anions; (**D**) Peptide chain length (n) dependences of the SOMO energies of the optimized C-terminal oligopeptide anions (opt) and the anions at their corresponding optimized neutral geometries (vert); (**E**) Dependences of VEAs of the neutral C-terminal oligopeptides and VDE of the C-terminal oligopeptide anions on dipole moments of the optimized neutral C-terminal oligopeptides and the corresponding neutral geometries after removing an electron vertically from the optimized C-terminal oligopeptide anions, respectively.

2. Calculational Details for Local Dipole Moments

To explain the localization phenomenon of excess electron around the curved oligopeptides, we define local dipole moment concept here by considering the following facts.

i) Although elongation of the oligopeptide chain increase dipole moment of the peptide chain considerably, further elongation can not increase the electron affinity or ability in binding an electron of the peptide chain after octapeptides (that is, longer than 8 peptide bond units), as shown in Figure 2.

ii) Excess electron does not always localize at the positive end of a dipole for all peptides, instead, at some zones which have large zone polarity.

iii) The cavity consisting of polar ligands to be used in capturing an excess electron is basically apolar, but it does effectively bind an excess electron. The more polar the cavity ligands in the solvated electron structure, the bigger the vertical detachment energy (VDE) of the bound electron, and the more stable the solvated electron.

iv) Bending can considerably increase electron affinity of a peptide chain at its bent or turn zone because the bending can considerably improve the dipole interaction between the adjacent peptide bond units (dipoles).

Thus, it is rational to assume that the local dipole moment is a dominant factor in binding an excess electron for peptides. However, no available schemes have been presented up to now for determination of the local dipole moment. Here, we propose a simple way to calculate it as the followings.

1) We roughly category a peptide chain into two parts: curved/bent and straight ones. The calculated distribution of an excess electron at a peptide chain indicates that the bent segment is the main residence for an excess electron, and thus is called as target segment which captures the "excess electron" and whose dipole moment is actually that of the local molecular fragment in the whole peptide chain and thus is defined as local dipole moment. The others are called the remaining segments.

2) The calculated distributions of excess electron for all considered peptide chains also reveal that the captured electron generally distributes at the N-terminal zone as possible (that is, some peptide bond units close to the N-terminal), and the short peptide chain linked to the N-terminal of the target segment using its C-terminal does hardly yield any effect on the binding of an excess electron, while that linked to the C-terminal can considerably contribute to increase of the dipole

moment and electron-binding ability of the target segment. Therefore, the target segment is defined as a segment starting from the excess–electron residing peptide bond unit being closest to the N-terminal and ending at a peptide bond unit close to the C-terminal. Generally, the target segment consists of 10-15 peptide bond units.

3) The target segments extracted from the peptide chains considered in this work are displayed in Figure S10 (**B**) and the cut bonds are saturated by the $–CH_3$ groups, and the calculated data are given in Figure S10 (**A**).

4) Calculations on these target segments give similar distributions of excess electrons and equivalent electron affinities to those about the whole peptide chains, but completely different dipole moment values, indicating this scheme for calculations of the local dipole moments is reasonable.

5) As shown in Figure 6, electron affinities of the peptide chains present a good correlation with the local dipole moments instead of the whole dipole moments.

3. Molecular Configurations of an Arbitrary Peptide Chain Used in Figure 6.

Conformations	**VEA**/eV	μ_{Total}/Debye	μ_{Local}/Debye
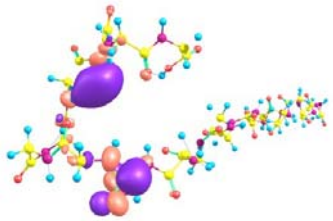	0.224	15.88	6.96
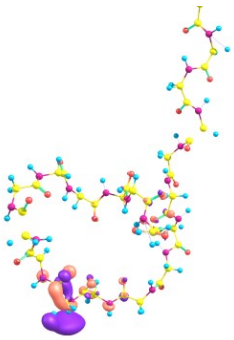	0.385	9.37	9.56
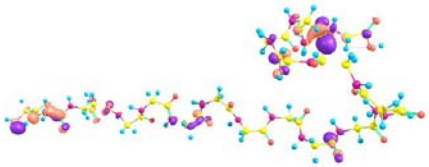	0.603	24.59	16.62
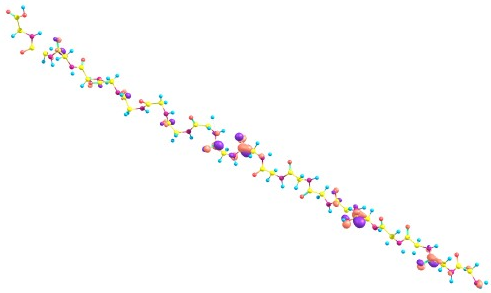	0.768	39.57	23.46
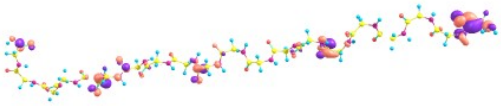	0.926	34.14	30.25
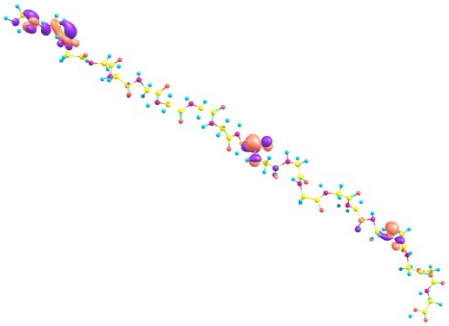	1.106	38.74	35.40

Figure S10 (A). The molecular orbitals and data correspond to the data points from left to right in Figure 6.

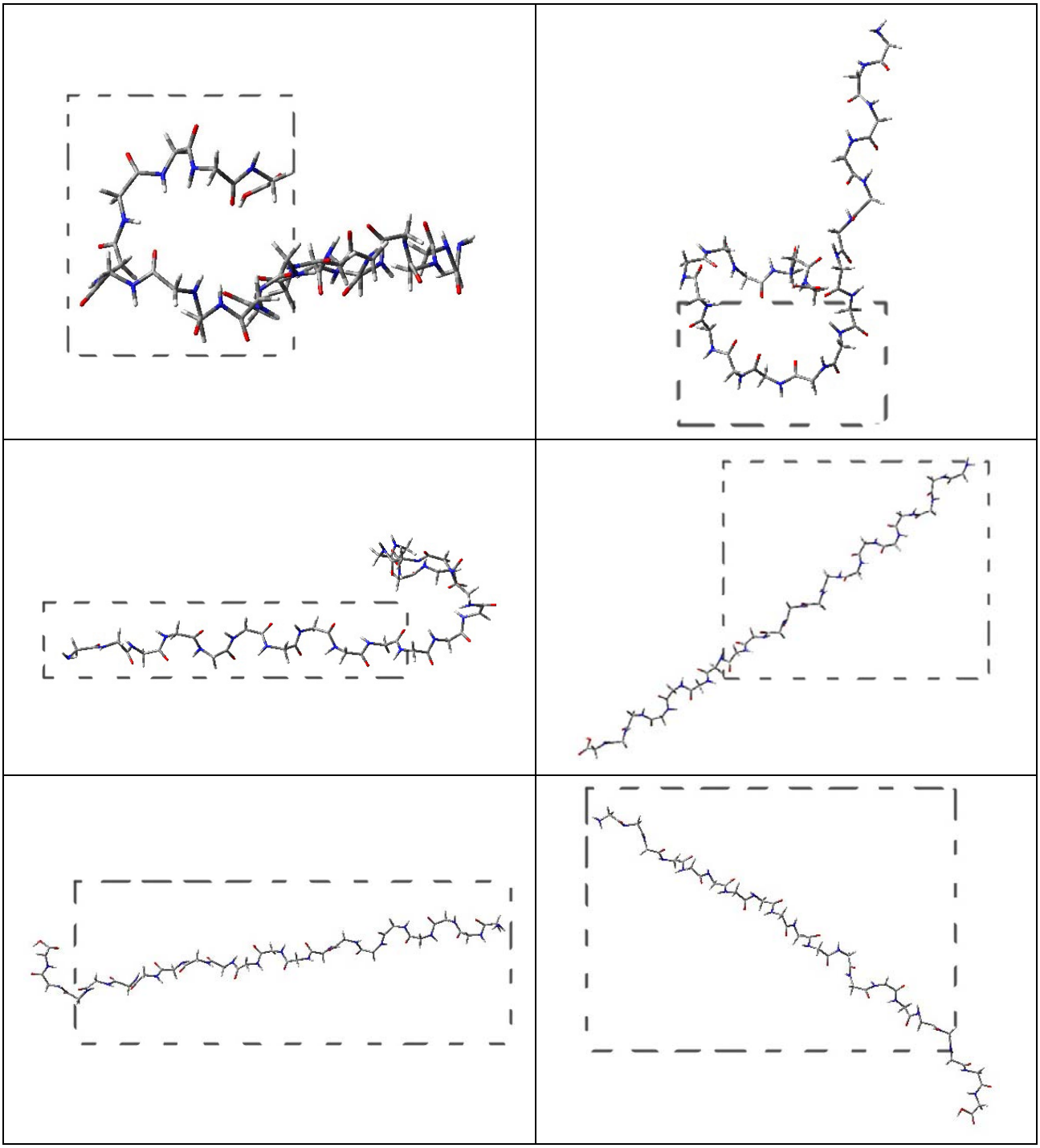

Figure S10 (B). The target segments extracted from six representative $(Gly)_{20}^{-}$ configurations, as marked by dash-lined boxes. The cut bonds are saturated by $–CH_3$ groups in the calculations of their local dipole moments.

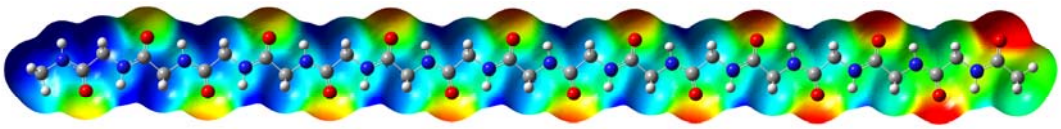

Figure S11. Electrostatic potential surfaces of a model 16-peptide ($H-(Gly)_{16}-CH_3$), indicating that the N-terminus could be the residing site of an excess electron.

4. The Calculated Data for α-Helices

Table S10. The adiabatic electron affinities (EA_a), vertical electron affinities (EA_a), vertical ionization potentials (IP_v), dipole moment (μ), and energies of LUMO for the α-$(G)_n$, α-$(G)_3KG^+_{n-4}$, α-$(G)_{n-1}K^+$, Ac-α-$(G)_{n-1}K$, α-$(G)_{n-1}KAc$ andα-$Ac(G)_{n-1}KAc^-$ obtained at the B3LYP/6-31++G(d,p)//B3LYP/6-31G(d) theory of level.

		5	7	9	11	13	15
α-$(G)_n$	EA_a(eV)	0.67	0.61	1.14	1.34	1.49	1.45
	EA_v(eV)	0.57	0.74	1.01	1.07	1.25	1.34
	IP_v(eV)	2.29	2.34	2.68	3.22	3.09	2.98
	μ(Debye)	18.30	27.08	37.87	47.62	58.12	68.46
	E_{LUMO}(eV)	-1.60	-1.77	-2.05	-2.11	-2.30	-2.40
α-$(G)_3KG^+_{n-4}$	EA_a(eV)	3.73	2.09	2.53	1.99	4.09	4.17
			3.81	3.90	3.96		
	IP_v(eV)	4.16	4.11	4.30	4.38	4.49	5.66
	μ(Debye)	33.10	16.58	29.34	27.07	81.00	89.28
	E_{LUMO}(eV)	-5.16	-3.47	-3.54	-3.41	-5.63	-5.66
α-$(G)_{n-1}K^+$	EA_a(eV)	2.42		1.97	1.60	1.97(3.17)	1.91(3.13)
	IP_v(eV)	3.78	3.72	3.67	3.57	3.51	3.48
	μ(Debye)	9.90	8.21	12.20	16.74	22.92	25.87
	E_{LUMO}(eV)	-3.40	-3.19	-3.08	-3.19	-4.57	-4.51
Ac-α-$(G)_{n-1}K$	EA_a(eV)	0.80	0.47	0.49	0.64	0.60	0.48
	EA_v(eV)	0.77	0.26	0.34	0.45	0.28	0.48
	μ(Debye)	10.80	15.51	19.39	10.12	16.18	9.17
	E_{LUMO}(eV)	-1.89	-1.21	-1.29	-1.36	-1.14	-1.34
α-$(G)_{n-1}KAc$	EA_a(eV)	0.81	0.73	1.22	1.48	1.65	1.78
	EA_v(eV)	0.65	0.74	0.93	1.08	1.28	1.36
	μ(Debye)	19.79	29.46	38.59	47.32	58.79	69.55
	E_{LUMO}(eV)	-4.25	-1.77	-1.96	-2.12	-2.34	-2.42
α-$Ac(G)_{n-1}KAc^-$	EA_a(eV)	-1.80	-1.70	-1.57	-1.47	-1.39	
	μ(Debye)	2.28	6.07	5.53	10.43	12.95	
	E_{LUMO}(eV)	0.99	1.03	1.02	0.96	0.79	

5. Geometries and Spin Density Distributions and All α-Helices

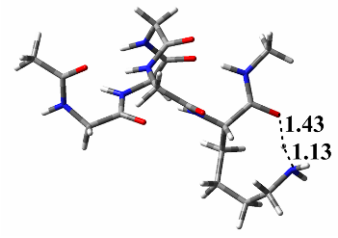

α-(Gly)$_4$K$^+$

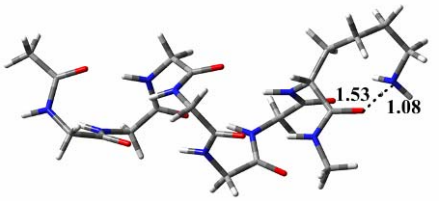

α-(G)$_6$K$^+$

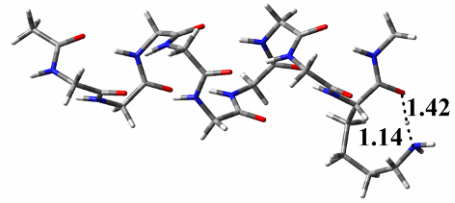

α-(G)$_8$K$^+$

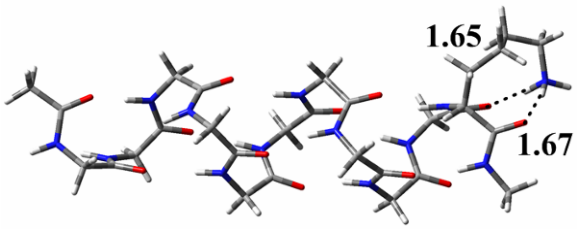

α-(G)$_{10}$K$^+$

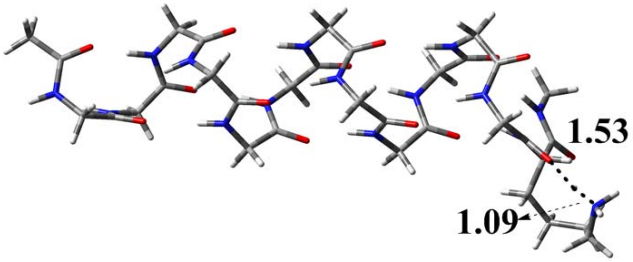

α-(G)$_{12}$K$^+$

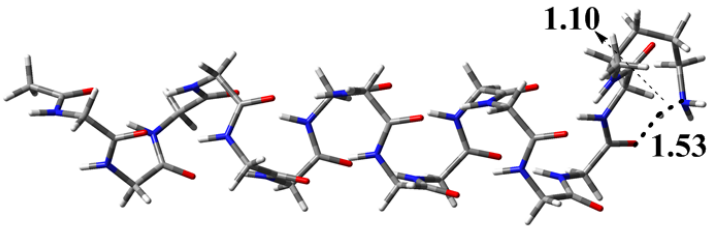

α-(G)$_{14}$K$^+$

Figure S12. The most stable structures of α-(G)$_{n-1}$K$^+$ (n=5~15). There are intramolecular H-bonds between the protonated side-chain of Lys and the C-terminal, which reduces the electron affinity of the protonated side-chain of Lys.

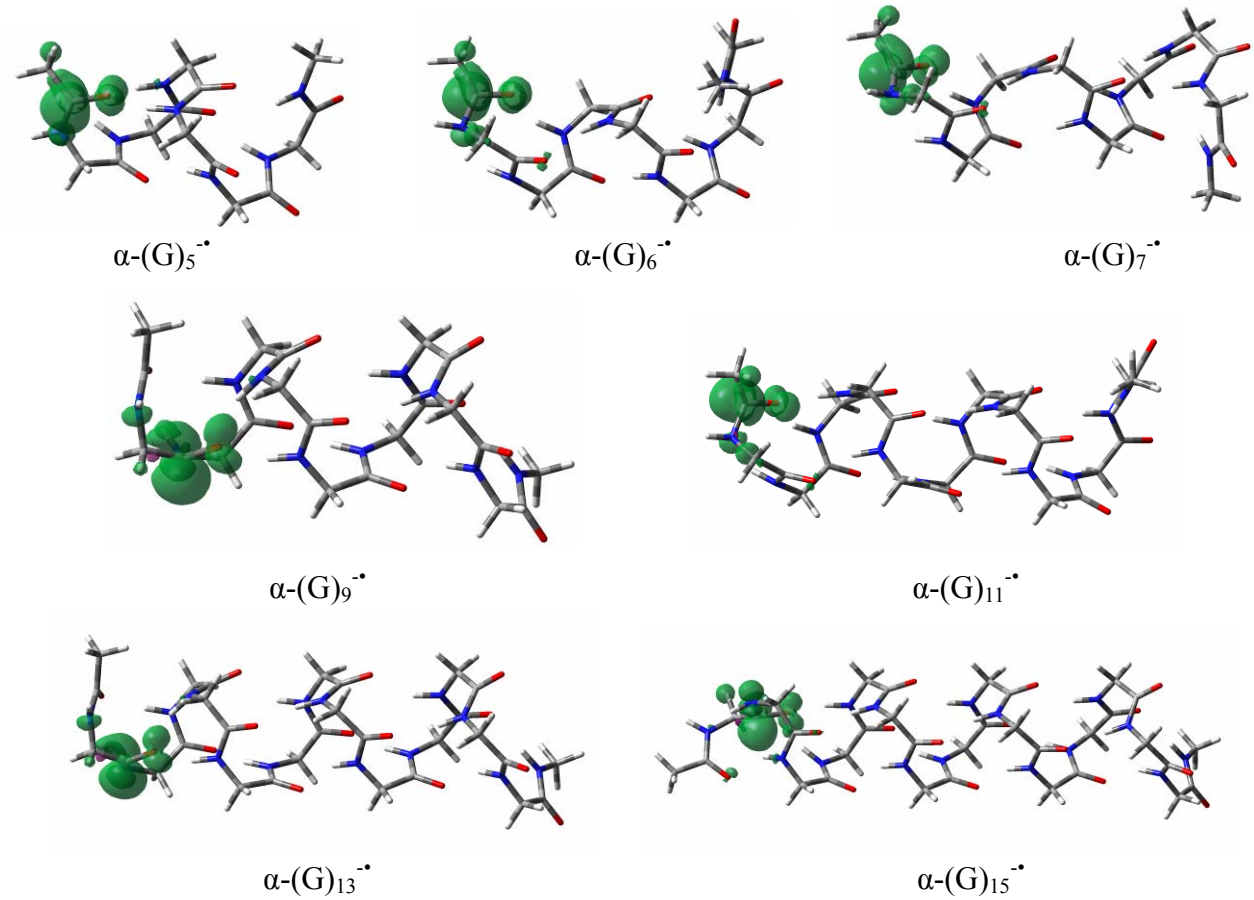

Figure S13. The distributions of the spin densities of α-$(G)_n^{-\bullet}$ (n=5~15).

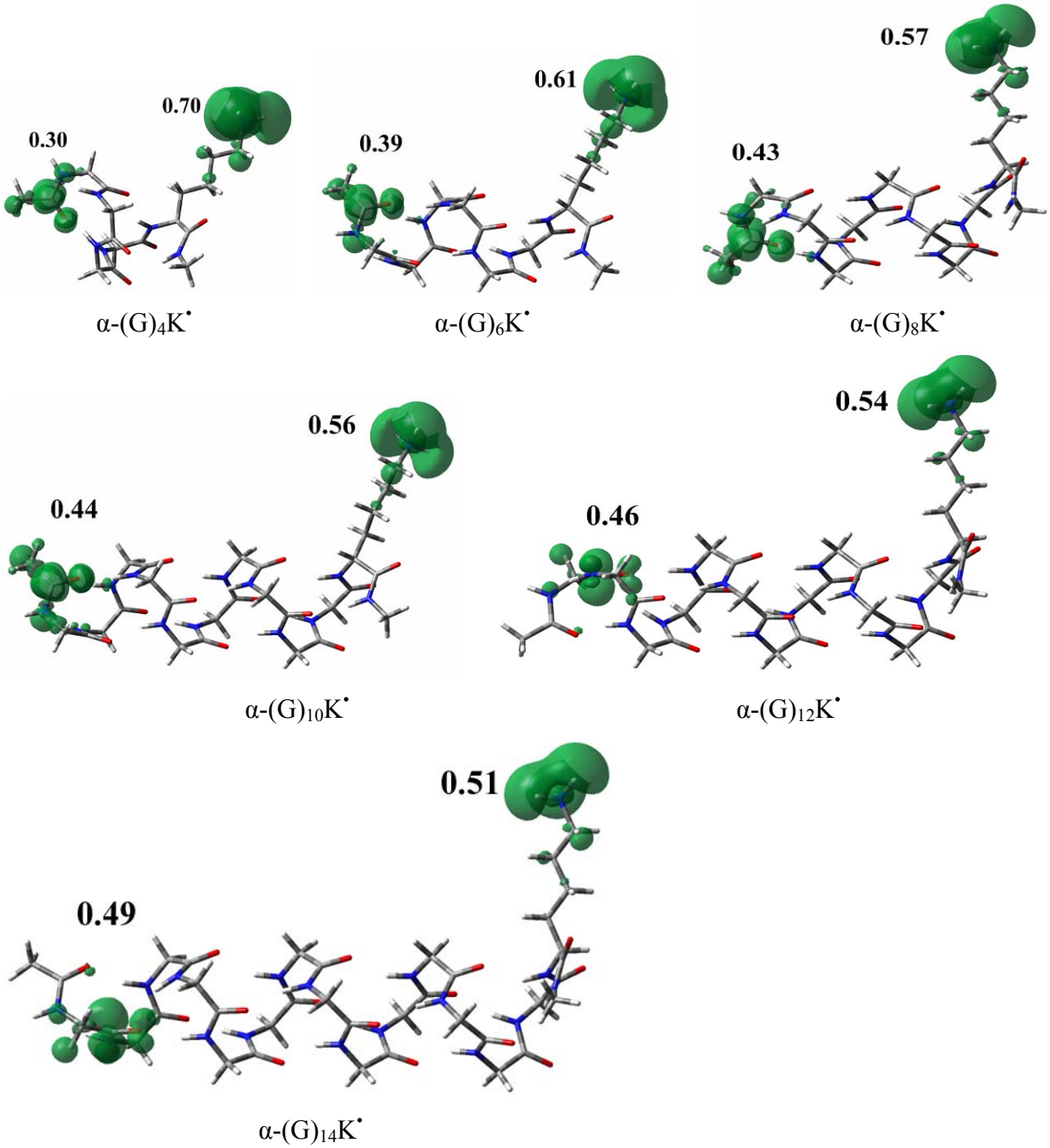

Figure S14. The distributions of the spin densities of α-$(G)_{n-1}K^{\bullet}$ (n=5~15).

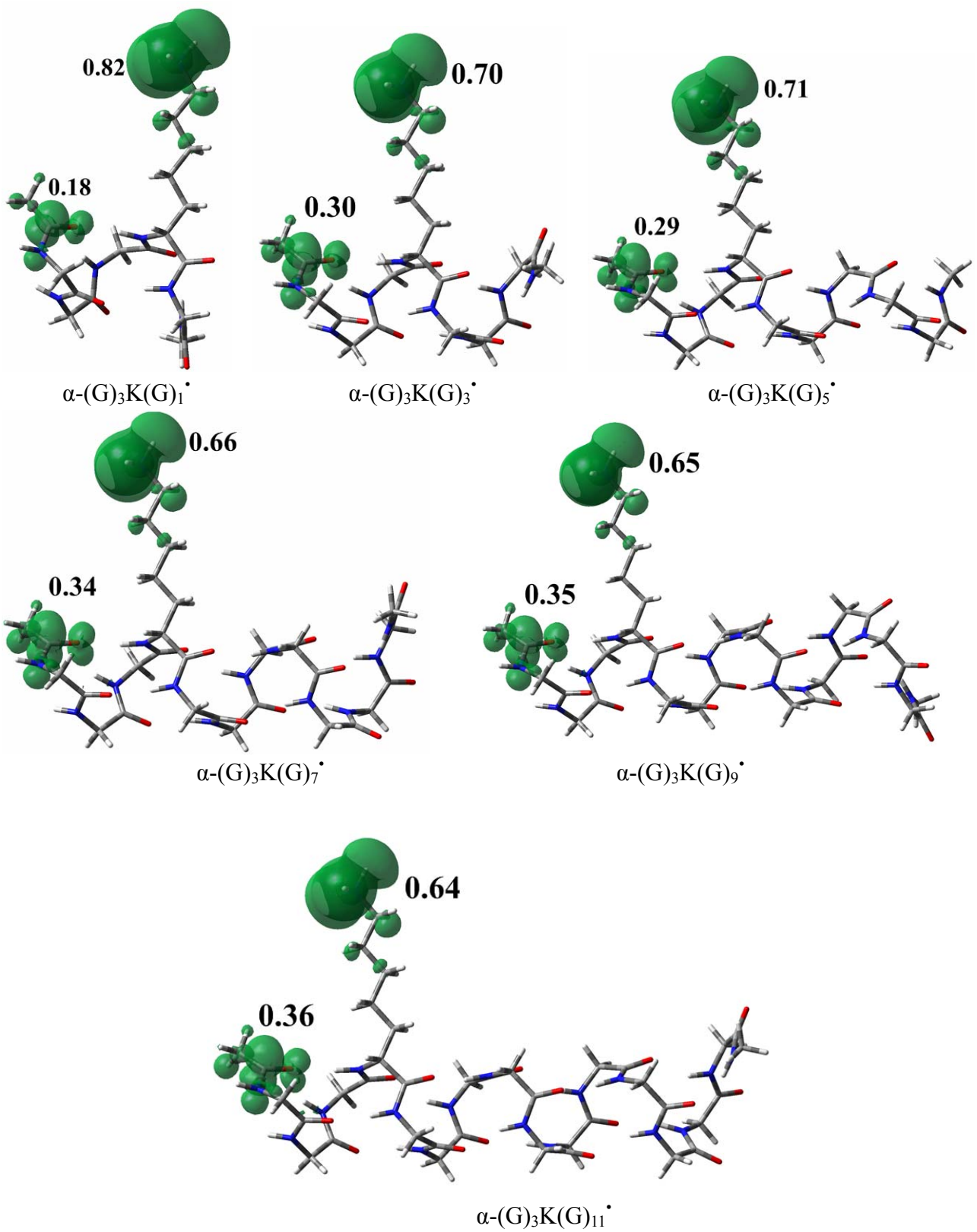

Figure S15. The positions of excess electron of α-$(G)_3K(G)_{n-4}^{\bullet}$ (n=5~15).

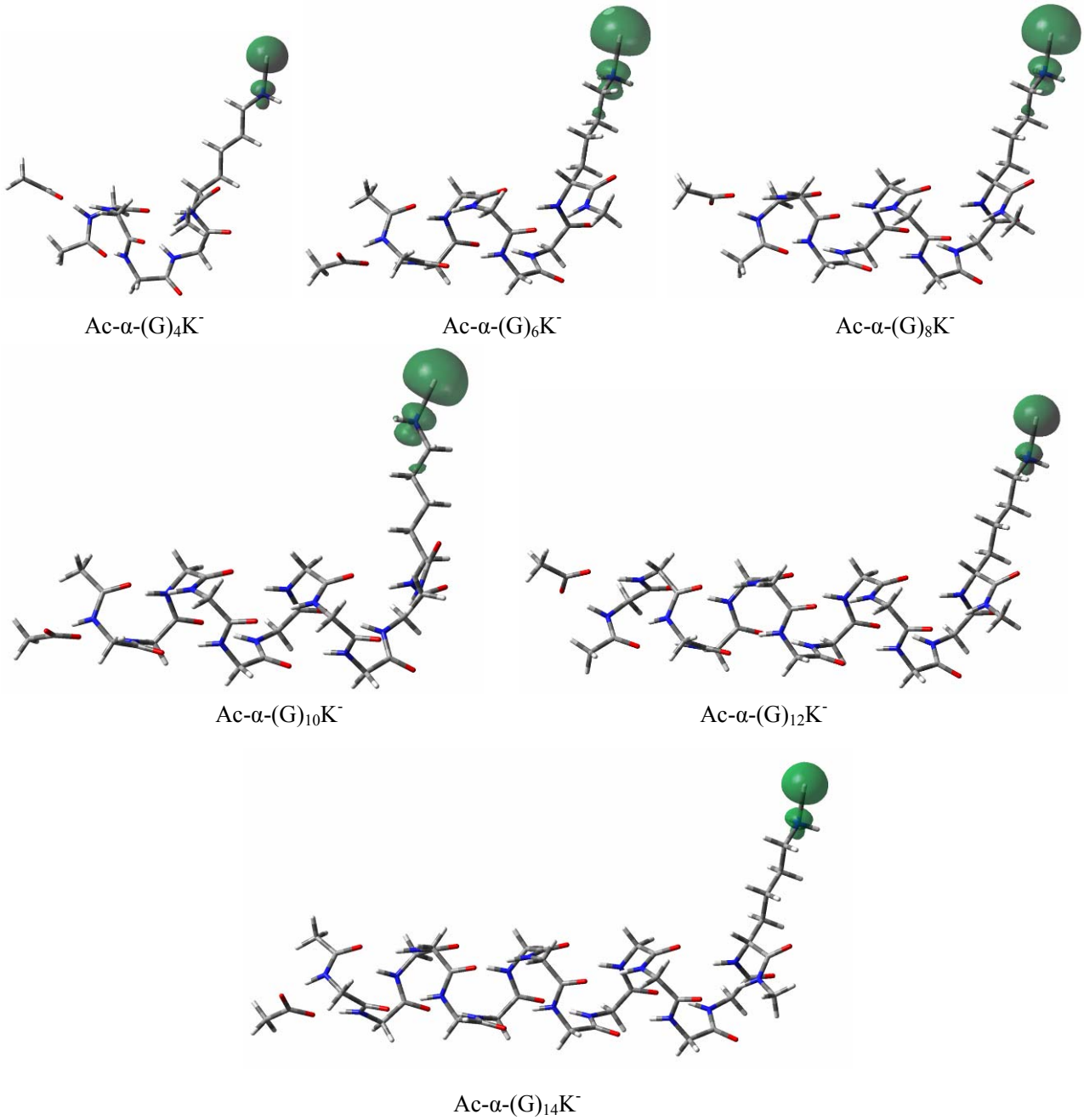

Figure S16. The effect of N-caps (deprotonated acetic acid, Ac^-) on the positions of excess electron of α-$(G)_{n-1}K^{\bullet}$ (n=5~15) were obtained at the B3LYP/6-31G(d) level of theory.

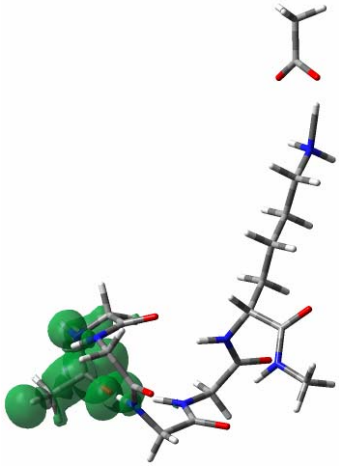

α-$(G)_4KAc^-$

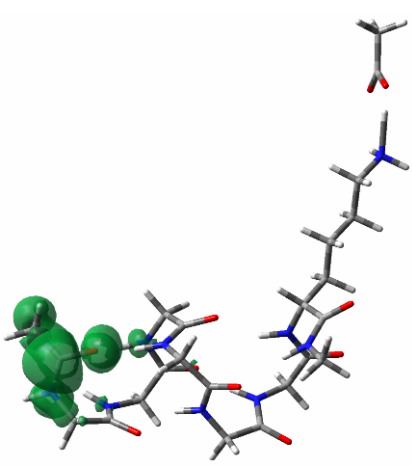

α-$(G)_6KAc^-$

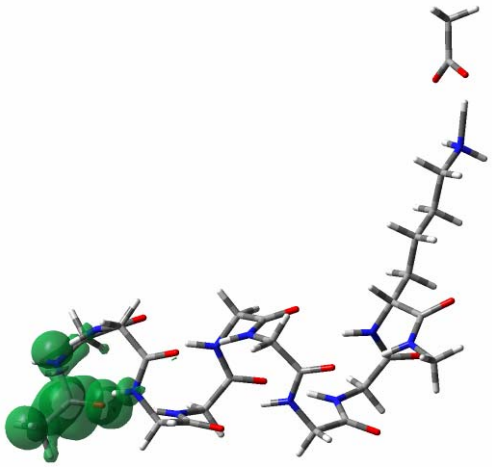

α-$(G)_8KAc^-$

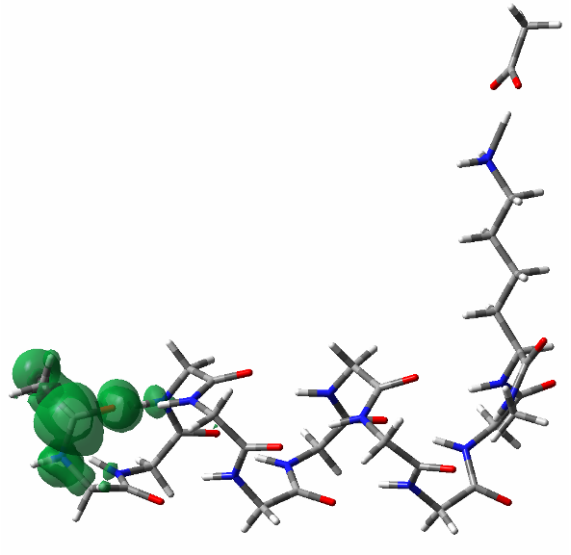

α-$(G)_{10}KAc^-$

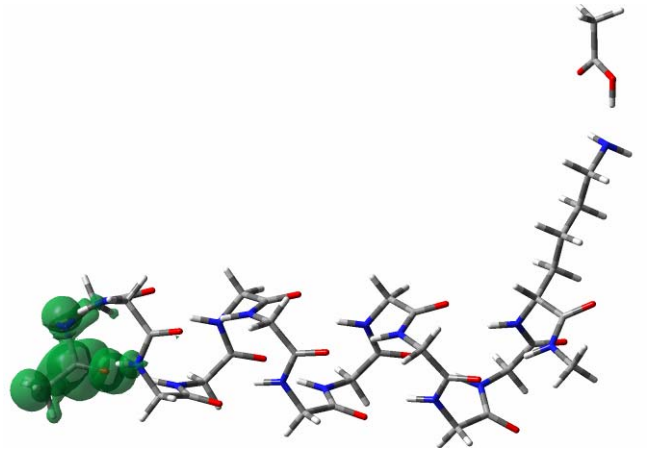

α-$(G)_{12}KAc^-$

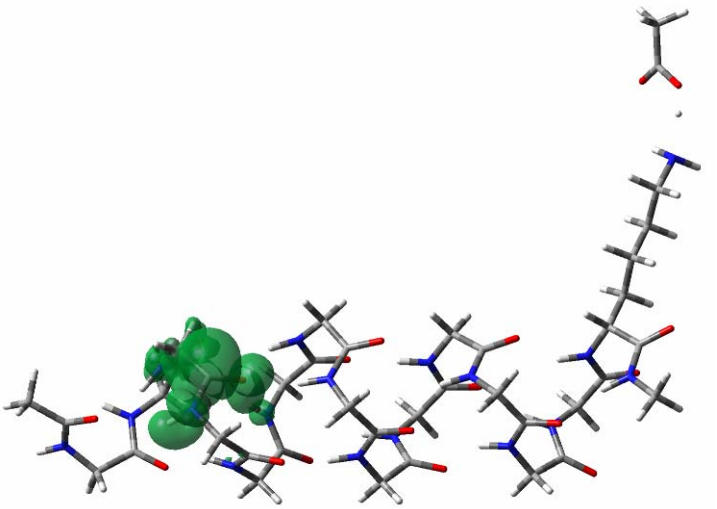

α-$(G)_{14}KAc^-$

Figure S17. The effect of a base (deprotonated acetic acid) approaching to the protonated side-chain of Lys (α-$(G)_{n-1}KAc^{-\bullet}$) on the positions of excess electron of α-$(G)_{n-1}K^{\bullet}$ (n=5~15) were obtained at the B3LYP/6-31G(d) level of theory.

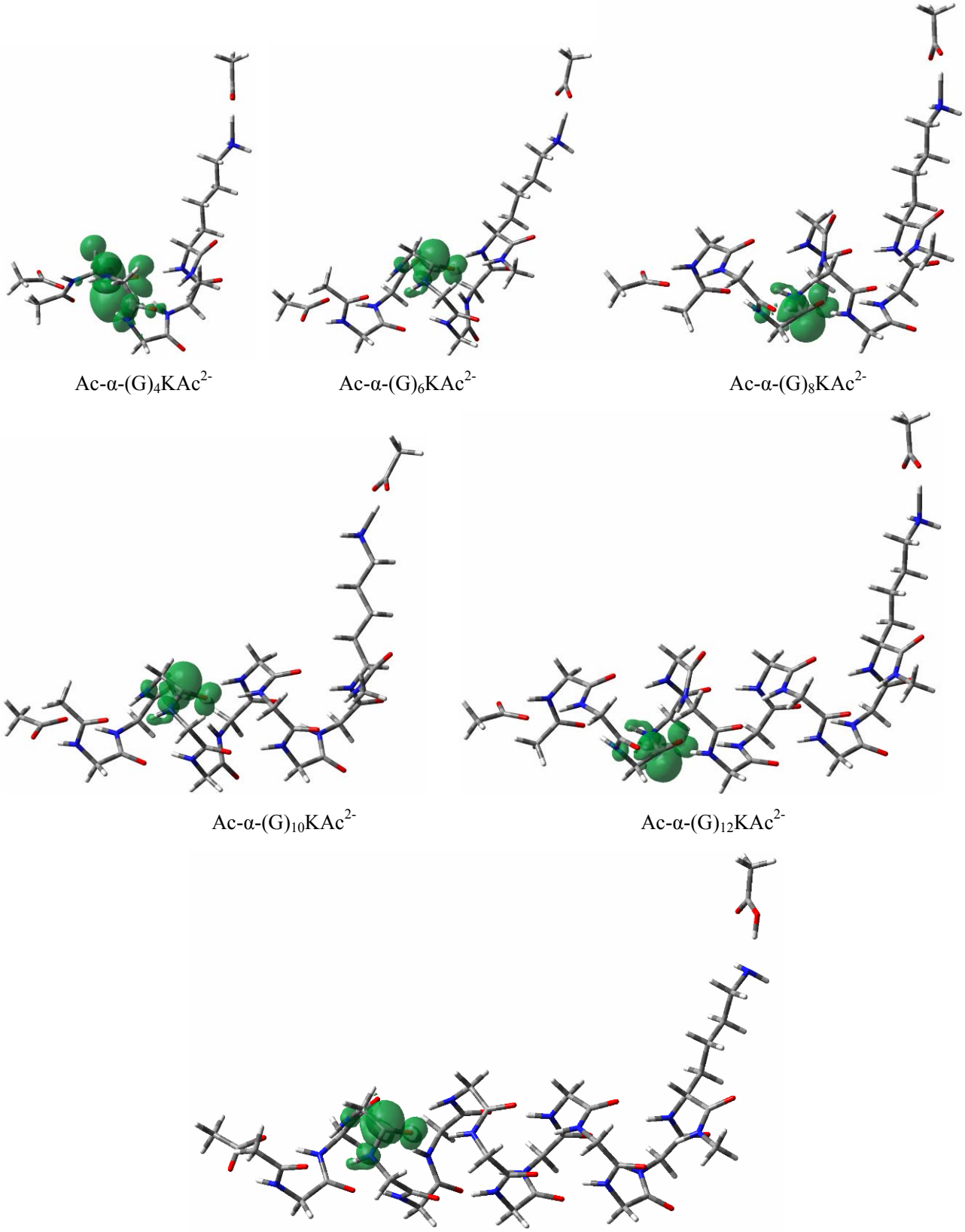

Figure S18. The effect of two base (deprotonated acetic acid) approaching to the protonated side-chain of Lys and N-terminus respectively (Ac-α-$(G)_{n-1}KAc^{2-}$) on the positions of excess electron of α-$(G)_{n-1}K^{\bullet}$ (n=5~15) were obtained at the B3LYP/6-31G(d) level of theory.

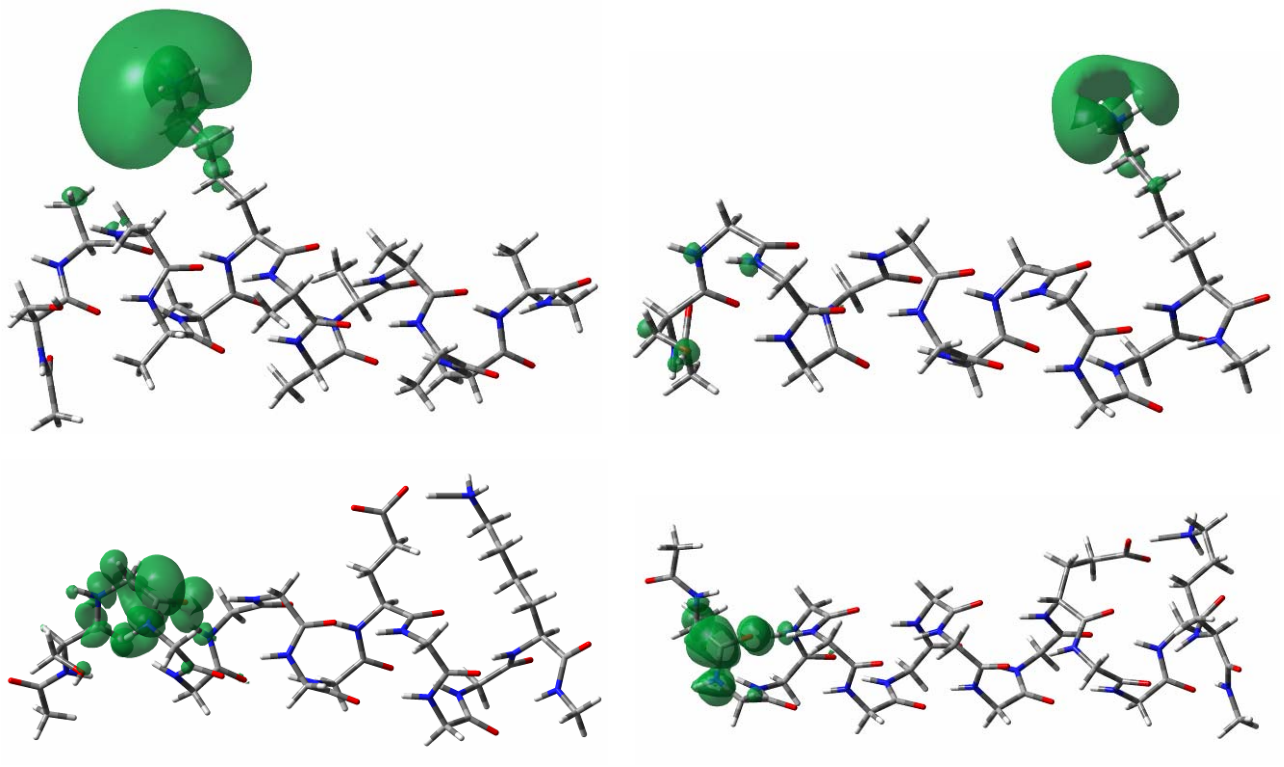

Figure S19. The effect of the side-chain of Ser as N-caps on the position of excess electron in the α-helixes (above two pictures) and the competition between the ethanol side-chain of Ser and the side-chain of Glu on the position of excess electron in the α-helixes.